A Deep Learning Approach to Predict Full-Field Stress Distribution in Composite Materials

Reza Sepasdar

Thesis submitted to the Faculty of the
Virginia Polytechnic Institute and State University
in partial fulfillment of the requirements for the degree of

Master of Science
in
Computer Science and Application

Anuj Karpatne, Chair
Maryam Shakiba, Co-chair
Lifu Huang

May 11, 2021
Blacksburg, Virginia

Keywords: Deep learning, CNN, Full-field prediction, Image-to-image translation, Adversarial learning

A Deep Learning Approach to Predict Full-Field Stress Distribution in Composite Materials

Reza Sepasdar

(ABSTRACT)

This thesis proposes a deep learning approach to predict stress at various stages of mechanical loading in 2-D representations of fiber-reinforced composites. More specifically, the full-field stress distribution at elastic and at an early stage of damage initiation is predicted based on the microstructural geometry. The required data set for the purposes of training and validation are generated via high-fidelity simulations of several randomly generated microstructural representations with complex geometries. Two deep learning approaches are employed and their performances are compared: fully convolutional generator and Pix2Pix translation. It is shown that both the utilized approaches can well predict the stress distributions at the designated loading stages with high accuracy.

A Deep Learning Approach to Predict Full-Field Stress Distribution in Composite Materials

Reza Sepasdar

(GENERAL AUDIENCE ABSTRACT)

Fiber-reinforced composites are material types with excellent mechanical performance. They form the major material in the construction of space shuttles, aircraft, fancy cars, etc., the structures that are designed to be lightweight and at the same time extremely stiff and strong. Due to the broad application, especially in the sensitives industries, fiber-reinforced composites have always been a subject of meticulous research studies. The research studies to better understand the mechanical behavior of these composites has to be conducted on the micro-scale. Since the experimental studies on micro-scale are expensive and extremely limited, numerical simulations are normally adopted. Numerical simulations, however, are complex, time-consuming, and highly computationally expensive even when run on powerful supercomputers. Hence, this research aims to leverage artificial intelligence to reduce the complexity and computational cost associated with the existing high-fidelity simulation techniques. We propose a robust deep learning framework that can be used as a replacement for the conventional numerical simulations to predict important mechanical attributes of the fiber-reinforced composite materials on the micro-scale. The proposed framework is shown to have high accuracy in predicting complex phenomena including stress distributions at various stages of mechanical loading.

Dedication

To my parents and sisters for their unconditional love and continuous support.

Acknowledgments

I would like to express my sincerest gratitude to my advisor, Professor Anuj Karpatne, for his support, guidance, and encouragement. I would like to extend my appreciation to my co-advisor, Professor Maryam Shakiba, for her unconditional support and for always encouraging me to follow my interest. I would like to thank my committee member, Professor Lifu Huang, for his constructive feedback and recommendations.

I would like to express my sincerest appreciation to my beloved family for their unconditional love, encouragement, and support. Seeing you happy has always been my greatest motive behind all my endeavors.

Contents

List of Figures

Chapter 1

Introduction

1.1 Motivation

High-performance continuous carbon fiber-reinforced polymer (CFRP) composites are material types that are light weight and have desirable mechanical performance. Hence, these composites are the material of interest in aerospace and automotive industries and are gaining traction in civil engineering applications to retrofit damaged structural members [3, 40]. CFRP composites are composed of unidirectional fibers with a certain orientation angle, embedded inside an epoxy matrix.

Engineering design of structures, constructed using CFRP composites, requires the knowledge of accurate mechanical properties of these materials. The mechanical properties of CFRP composites, in turn, depends on the geometry of their microstructures, and hence obtaining them requires simulations on the micro-scale. In the simulations, a small portion of the microstructure, called representative volume element (RVE), is simulated under mechanical loading. These simulations also provide information about the damage and failure mechanisms, the knowledge of which is crucial for a better understanding of the mechanical behavior as well as for any possible improvement in these material types.

The only available tool to conduct such simulations is the finite element (FE) method. This method, however, is numerical and highly computationally expensive. Therefore, FE sim-

ulations of materials with complex geometries (e.g., composite materials' microstructures) are significantly time-consuming, even when run on a supercomputer. Also, a robust simulation of damage and failure of the composite materials requires the implementation of accurate constitutive equations for different constituents of the microstructure. The constitutive behaviors for modeling damage and failure of materials are complex and do not have straightforward implementations.

Hence, due to the aforementioned downsides of the FE method, there is a great interest to reduce the complexity and computational cost while maintaining the accuracy of the simulations. This study proposes a deep learning framework as a surrogate for the conventional costly FE simulations. The proposed framework is able to predict complex mechanical attributes of CFRP composites with high accuracy.

1.2 Problem

The CFRP composites have large stiffness and load-carrying capacity when loaded along the fibers direction, as demonstrated in Figure 1.1a. These composites, however, are not as strong and stiff under loading transverse to the fibers' direction. Since these composites are subjected to multi-axial loading in practice, the initiation of damage is characterized by cracks formation transverse to the fibers' axis, as shown in Figure 1.1b. As a result, the transverse properties of CFRP composites significantly affect the overall mechanical behavior and it is crucial to better understand them. Hence, the transverse behavior of CFRP composites has been the subject of several research studies in the past few decades (e.g., [23, 27, 31, 37, 38, 41, 45]). The only approach to study the transverse full-field attributes (e.g., stress distribution and damage propagation) of CFRP composites is the FE method.

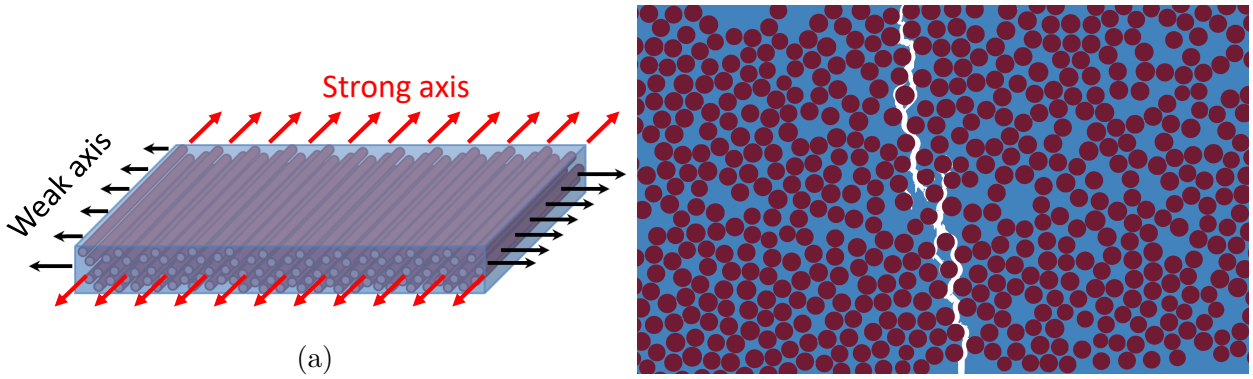

(a) (b)

Figure 1.1: Illustrations of (a) weak and strong axes in CFRP composites and (b) a transverse crack resulting from loading along the weak axis.

The FE simulation of continuous CFRP composites' transverse behavior are normally conducted using two-dimensional (2-D) numerical models where all the constituents (i.e., fibers, matrix, and fibers/matrix interfaces) are explicitly modeled within an RVE, containing randomly distributed fibers (e.g., [7, 13, 21, 24, 26, 33, 48, 50]). The complex geometry and implementation of accurate damage constitutive equations makes both the implementation process and analysis time-consuming.

In order to overcome the computational cost, this study proposes a deep convolutional neural networks (CNN) framework to predict full-field stress distribution at the elastic stage (before initiation of damage) and at an early stage of damage initiation (ESoDI). The knowledge of these attributes can provide information necessary for the mechanical design and a better understanding of the mechanical properties of CFRP composites. The proposed framework is designed to be simple and learns to make predictions only based on the microstructural geometry as the input. After the framework is trained, it can predict the aforementioned attributes instantaneously.

1.3 Research Question

Can CNN learn the complex local and global morphological features in the composites microstructures that are significant predictors of the stress distributions at different loading stages? In terms of accuracy and ease of use, what deep learning technique would have a better performance?

1.4 Hypothesis

In order to solve the research problem answer the above mentioned research questions, the following hypothesis is presented: Development of an efficient deep learning framework can overcome the complexity and computational cost associated with the FE simulations of CFRP composites under mechanical loading.

1.5 Contribution

In this thesis, a deep learning framework is proposed as a surrogate for the expensive FE simulations of CFRP composite materials. The contribution of this research is highlighted as follows:

- Several microstructural representations for the CFRP composites are synthetically generated and simulated within an efficient FE framework, and a sufficiently large data set is generated
- A deep learning framework is proposed and trained using the results of FE simulated RVEs to predict full-fill stress distributions at various loading stages.

- The proposed deep learning framework is trained to translate the microstructural geometry to the full-field stress contours at elastic and ESoDI loading stages.
- Two popular techniques in translating representations are employed as the deep learning framework and their performances are compared.

1.6 Organization

This manuscript is organized as follows: Chapter 2 briefly presents a previous research study by the author that motivated this thesis. Chapter 3 includes a literature review with a focus on research studies that utilized deep learning approaches to predict various mechanical attributes of solid materials. Chapter 4 explains the data generation and preparation processes and presents the deep learning approaches utilized to translate the microstructural geometry of CFRP composites to the full-field stress distribution as various loading stages. Chapter 5 presents the results and discusses the performance of the utilized deep learning methods. Chapter 6 summarizes the proposed approaches and presents the research findings. It must be noted that in the rest of this manuscript, the word "stress" always refers to "von Mises stress"; we simply omit the term "von Mises".

Chapter 2

Motivating Work

This research was motivated by the findings of an earlier research study by the author. Sepasdar et al. [34] proposed an image-based deep learning framework to generate an image of full-field stress contours at an ESoDI based on an image of the microstructure. The microstructural geometry of the studied RVEs were complex, including 46 randomly distributed fibers. ESoDI was a loading stage immediately after the initiation of the transverse crack, when the resistance was decreased by 5%. They showed that the stress distribution at this stage can determine the ultimate crack pattern in the microstructural representations of CFRP composites. Hence, they trained another network to predict the crack pattern based on the predicted image of stress distribution at the ESoDI loading stage. The proposed framework by Sepasdar et al. [34] was able to predict the failure pattern with high accuracy.

2.1 Pros and Cons of the Method Proposed By Sepasdar et al. [34]

The framework proposed by Sepasdar et al. [34] is convenient to train by the user since it is trained using the images of attributes such as microstructural geometry and stress distribution. Recording these attributes in image formats is an straightforward task in any commercial FE software. The framework, however, does not generate the actual values of

stress and only generates an image of the stress contours. Although the images of stress distributions at ESoDI can provide enough visual information for a second network to accurately generate the crack patterns, visually extracting the actual stress values at different zones of the image is inconvenient and can be inaccurate. Other tasks, such as engineering design of the CFRP composites, require the knowledge of the precise values of stress. Also, Sepasdar et al. [34] used a fully convolutional generator in their framework and did not test the performance of more advanced image-to-image translation techniques. Moreover, Sepasdar et al. [34] did not attempt to generate the stress distribution in the elastic loading stage, the knowledge of which is crucial for the engineering design purposes.

2.2 Improvements Offered by This Research

This research builds upon a previous work by Sepasdar et al. [34] to improve its capabilities and address its above-described shortcomings. Hence, the framework proposed in this research aims to generate the actual values of full-field stress distribution based on the microstructural geometry. This research also attempts to predict the full-field stress distribution at the elastic loading stage in addition to the stress distribution at the ESoDI loading stage. Moreover, this research employs an advanced image-to-image translation technique (i.e., Pix2Pix translation [17]) and compares its performance with that of a fully convolutional generator approach. Since, the framework proposed in this research is non-image-based, the process of data preparation requires additional efforts, as is explained in Section 4.4. Hence, the proposed framework complements the one proposed by Sepasdar et al. [34] and provides the user with options on which framework to use based on the application.

Chapter 3

Review of Literature

The application of deep learning in the area of computational solid mechanics is at an early stage of research. The majority of the studies in the literature used deep learning to predict one-dimensional attributes, describing the overall mechanical behavior and constitutive laws of heterogeneous materials on the meso-scale and structure level [5, 12, 14, 25, 42, 43, 44]. Full-field predictions of attributes including damage and stress distribution of materials is scarce in the literature and only the problems with simple geometries were studied.

Utilizing deep learning techniques to predict failure pattern and full-field stress distribution in composite materials with complex microstructural geometries, in the presence of damage and nonlinearity, were recently attempted by Sepasdar et al. [34]. They proposed an image-based deep learning framework to to predict crack pattern and generate full-field stress contours in the presence of damage. This thesis builds upon the proposed method by Sepasdar et al. [34] to generate the actual values of stress distribution and make predictions in a non-image-based manner.

In the subsection below, the existing research studies on the application of deep learning to predict full-field stress distribution as well as damage and failure of solid materials are reviewed. It must be noted that except for the fully physics-based approaches, all the proposed deep learning frameworks in the literature were trained using data sets generated from FE simulations.

3.1 Full-Field Stress Prediction in Materials

The application of deep learning in predicting full-field attributes of materials such as stress distribution, resulting from an applied mechanical load, is quite scarce in the literature. Also, only the materials with simple geometry were considered and the predicted stress distribution was limited only to the stages of loading where damage was not present.

Donegan et al. [8] utilized CNN to predict the locations of stress localization due to thermal loading in 2-D representations of fiber-reinforced composites. Although, the RVEs were complex and included multiple fibers, the proposed framework was only able to predict the locations of stress hot spots and not the actual values of stress. In other words, the pixels of the generated image could take on binary values corresponding to hot spot and non-hot spot stresses. Feng and Prabhakar [10] predicted elastic stress distribution in 2-D representations of fiber-reinforced composite materials. The studied RVEs were small, containing four fibers.

Physics-based machine learning was also utilized in the area of solid mechanics to predict full-field stress distribution of materials with simple geometries [2, 11, 47]. In these approaches, the cost function is designed based on the governing laws in computational solid mechanics. The training of these framework does not requires supervision and is solely guided by the cost function. The physics-based methods, however, requires designing and implementing robust and complex objective functions, achieving which is not simpler than FE formulation and implementation. Also, the functionality of the physics-based techniques in predicting full-field stress distribution, damage, and failure of materials with complex geometries is yet to be studied.

Sepasdar et al. [34], proposed a deep learning framework to predict an image of the full-field stress contours of particulate composite materials in the presence of damage. The proposed framework was briefly explained in Chapter 2.

3.2 Damage and Failure Prediction in Materials

The application of deep learning to detect damage and failure in materials has been substantially studied by several researchers and major progresses have been made (e.g., [9, 19, 20, 28, 36]). However, the application of deep learning techniques in predicting damage and failure pattern of materials is scarce in the literature and only simple problems were studied. Hunter et al. [15] used deep learning to predict crack pattern in brittle geomaterials. The training data was generated using FE simulations of several concrete wall specimens subjected to tension. Each concrete wall specimen included 20 identical pre-existing cracks, randomly distributed within the wall. A number of geometrical features were engineered as the predictors of the failure pattern. The utilized network had a simple architecture to avoid overfitting. The proposed framework had an acceptable performance in predicting the crack path.

Schwarzer et al. [32] used similar sample specimens as Hunter et al. [15] study to predict the evolution of fracture in brittle materials. However, they used a different ML approach. Instead of manually defining the features for the deep learning framework, a CNN was used to extract the significant features. The features were then fed to a recurrent neural network to predict the evolution of fracture over time. The proposed approach was shown to have acceptable accuracy. Pierson et al. [29] employed a CNN to predict the topography of the crack surface in polycrystalline alloys. The predictions were based on the microstructural geometry and the prior knowledge of the crack surface location. The method used a simple network architecture and hence, the predictions could not reach a high accuracy.

Sepasdar et al. [34] proposed a deep learning framework to predict the failure pattern of particulate composite materials with complex microstructural geometries. The reader can refer to Chapter 2 for a brief explanation of the framework and findings.

Chapter 4

Methodology

In this chapter we present a deep learning framework to predict full-field stress distribution in 2-D representations of CFRP composite materials based on the geometry of microstructures. The framework is capable of generating the stress distribution at various loading stages.

4.1 Overview

Several RVEs of CFRP composites with complex geometries are generated and simulated under mechanical loading using an efficient FE framework to provide the required training and validation data sets. A fully convolutional network is designed to input the microstructural geometry and generate the stress distribution as the output in the form of a matrix, containing the actual values of stress at different locations of the RVE. The output matrix is similar to a grayscale image in which the pixels contain the actual stress values instead of RGB or grayscale color values. Two generator networks with the same architecture are trained, in a supervised fashion, to generate:

- Full field stress distribution at an elastic loading stage (Target 1) based on the microstructural geometry (Input). The elastic stage corresponds to any loading step before the non-linearity and damage are present.

- Full field stress distribution at an ESoDI loading stage (Target 2) based on the mi-

crostructural geometry. At this stage, the failure has initiated, damage and non-linearity are present, and the resistance is decreased by 5%.

A more precise definition of the above described loading stages are presented in Section 4.3 and the importance of those stages is discussed. Two different techniques for the training of the generator networks are considered and their performances are compared:

- Training by using a simple mean absolute error (MAE) objective function for the generator network.

- Training in an adversarial fashion through a Pix2Pix translation scheme [17].

The different considered training scenarios are explained in detail in Section 4.5

4.2 Representative Volume Elements

A random fiber generator algorithm developed by Sepasdar et al. [34] was used to generate several 2-D microstructural representations of the CFRP composite. The algorithm randomly distributes the fibers within an RVE based on a target distribution for the fibers nearest neighbour distances (NND). 4500 RVEs were generated based on a target distribution for the fibers' NND, measured using an experimental image of a CFRP microstructure [22, 46]. The generated RVEs had fixed dimensions of $54\mu m \times 54\mu m$ and contained 46 identical fibers with a diameter of $7\mu m$. An example of a generated RVE and the comparison between its fibers NND distribution and that measured experimentally is illustrate in Figure 4.1.

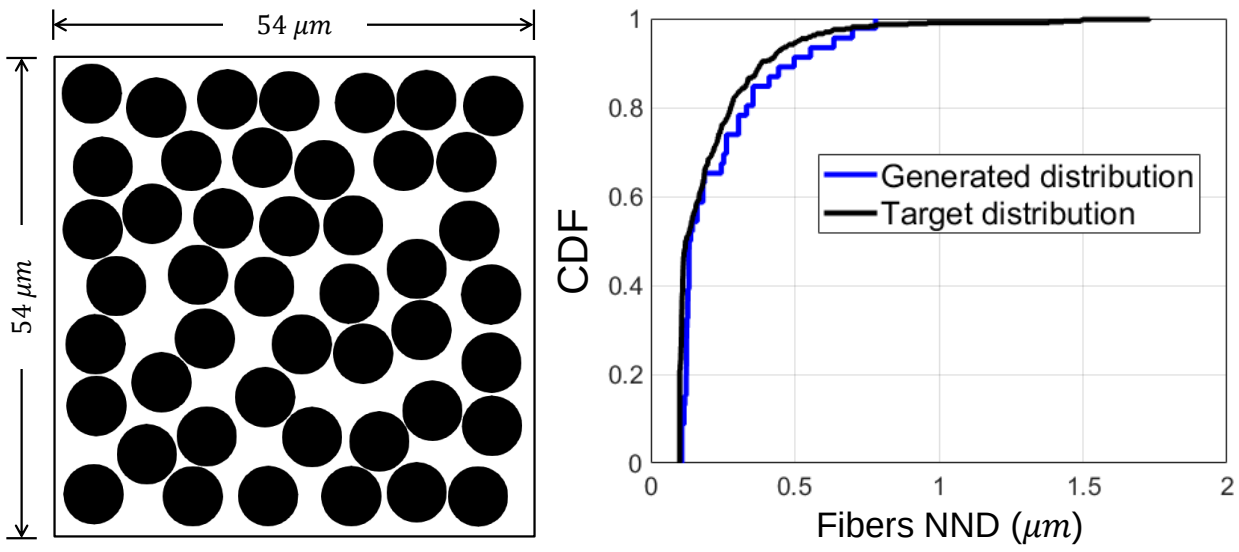

(a) (b)

Figure 4.1: (a) Illustrations of a generated RVE and its dimensions and (b) the comparision between the generated and target distributions of fibers' NND

4.3 Finite Element Simulation

The mechanical behavior of the generated RVEs were simulated using a developed efficient FE framework [13, 35]. The FE framework was programmed in C++/MPI environment and was designed to run the simulations in parallel. In FE simulations, the geometry of the numerical models needs to be meshed using several finite elements, as illustrated in Figure 4.2a. The response of the numerical model to the applied mechanical loading is calculated at the nodes of the elements, as depicted in Figure 4.2b.

The RVEs were then subjected to transverse tensile loading under plane-strain, displacement control conditions, as illustrated in Figure 4.3a. The loading was applied incrementally in 100 steps and for each step, the global load-displacement response and nodal stresses were recorded. An example of a typical load-displacement response is illustrated in Figure 4.3b. As seen in the figure, the initial portion of the response is linear. At this loading stage, no damage or crack is present and the matrix, fibers, and fiber/matrix interfaces are intact. The

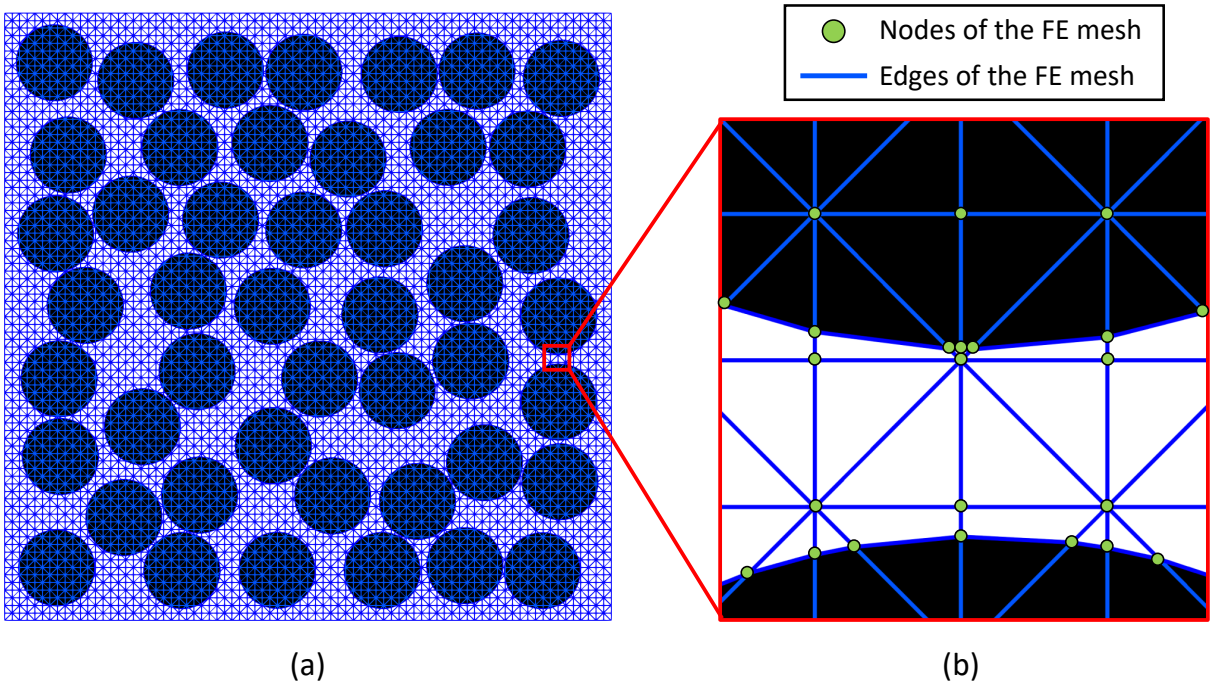

Figure 4.2: Illustration of (a) FE mesh and (b) edges and nodes of the FE mesh.

initial linear portion is referred to as the elastic loading stage. At this stage, the magnitude of stress at every location in the geometry is proportional to the loading. In other words, if for each loading step, we normalize the stress distribution based on the maximum stress value in the RVE, the resulting normalized stress distribution does not change so long as the loading is within the linear elastic range. As loading increase, the behavior gradually becomes non-linear due to the formation of damage and micro-cracks within the numerical model. The load keeps increasing until the maximum resistance (F_{max}) of the RVE is reached. After this point, the induced damage and micro-cracks quickly propagate towards the top and bottom boundaries and the resistance starts to decrease. When the transverse crack is completely formed across the RVE (Figure 1.1b), the resistance drops to zero, marking the complete failure of the composite.

The stress distributions at two important loading stages are:

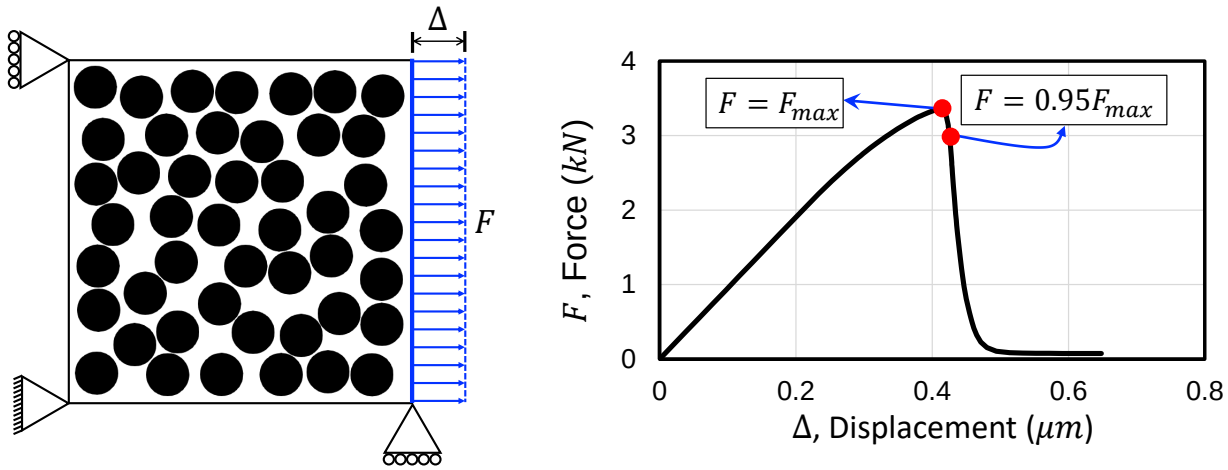

(a) (b)

Figure 4.3: FE simulation: (a) the boundary conditions imposed to the edges of the RVEs and (b) a typical force-displacement response of the simulated RVEs, illustrating the maximum force and the force at ESoDI stage of loading.

- The stress distribution at the elastic stage which specifies the locations of stress concentrations in the RVE that are more susceptible to damage. An example of a typical normalized stress distribution at the elastic loading stage is depicted in Figure 4.4a.

- The stress distribution at ESoDI which we define as a loading stage where the resistance is decreased by 5%. This stage of loading determines the locations of damage initiation and how the induced damages impact the elastic stress distribution. Sepasdar et al. [34] showed that stress distribution at ESoDI also hints the pattern of the ultimate crack at the end of loading. A typical example of stress distribution at ESoDI is illustrated in Figure 4.4b.

The knowledge of stress distribution at the aforementioned loading stages can provide valuable information regarding engineering design of CFRP composites. Therefor, we recorded the stress distribution at the elastic and ESoDI loading stages with the aim of training a deep learning framework, able to generate stress distributions at those loading stages based on the microstructural geometry.

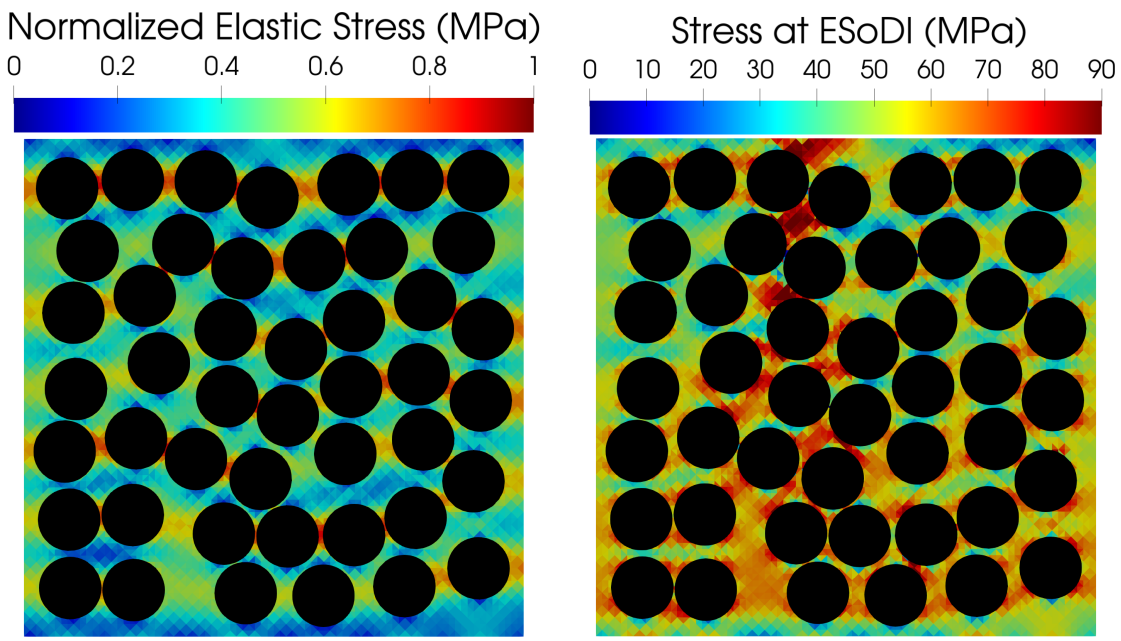

(a) (b)

Figure 4.4: Typical examples of (a) normalized elastic distribution and (b) stress distribution at the ESoDI loading stage.

The required resources to run the FE simulations of the 4500 generated RVEs were provided by Advanced Research Computing at Virginia Tech. The total run-time was 12 days using a 2×Intel Xeon E5-2680v3 CPU with 24 processors. The results were then undergone a pre-processing step to be converted to an appropriate format, required by the deep learning framework.

4.4 Data Pre-Processing

The output stress contours from the FE simulation frameworks were saved in the VTK format. An open-source visualization application named ParaView was used to read and process the VTK files. It is reminded that in FE simulations, the stress values are evaluated at the nodal points of the FE mesh and because of the complex geometry, the nodal points are

not uniformly distributed in the form of regularly separated grids. This point is schematically illustrated in Figure 4.5a.

To be able to take advantage of convolutional layers to capture the significant geometrical features of the microstructure, the inputs and outputs of the network should be in the form of regularly separated grids, presented in the form of a 2-D tensor. Hence, the results needed to be converted to a uniformly separated grids. This task was achieved via an available function in ParaView, namely, Resample To Image, which performs the conversion through interpolation among neighbouring data points. This function was used to convert the representation of data from a point cloud to a 256×256 grid, as depicted in Figure 4.5b.

To simplify the representation of the microstructural geometry, the areas occupied by the fibers were assigned a value of 0 while the other areas were assigned a value of 1. Both the geometrical and stress distributions were saved in the form of CSV files. In summary, each data sample contained three CSV files representing microstructural geometry (Input), elastic stress distribution (Target 1), and stress distribution at ESoDI (Target 2).

The 4500 processed data samples were then separated in mutually exclusive training and validation data sets, containing 4000 and 500 data samples, respectively. To further increase the robustness of the training data set, all of the the training samples were flipped vertically as a simple data augmentation technique.

4.5 Deep Learning Framework

In this section, the deep learning approaches employed to translate the microstructural geometry (Input) to elastic and ESoDI stress distributions are explained (Target 1 and Target 2). It must be noted that the predictions of stresses at elastic and ESoDI loading stages are

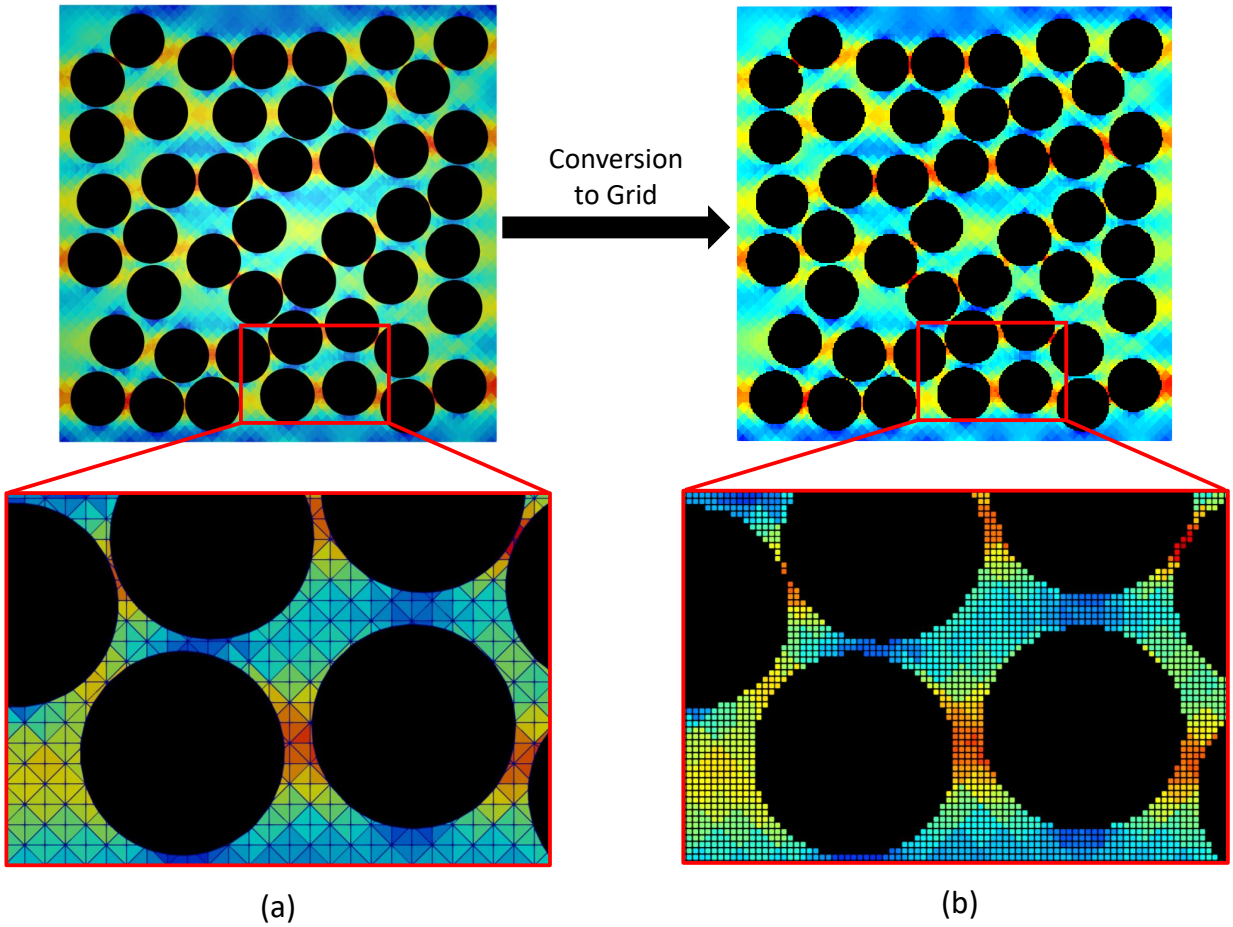

Figure 4.5: Conversion of the FE generated data from FE mesh to uniformly separated grids.

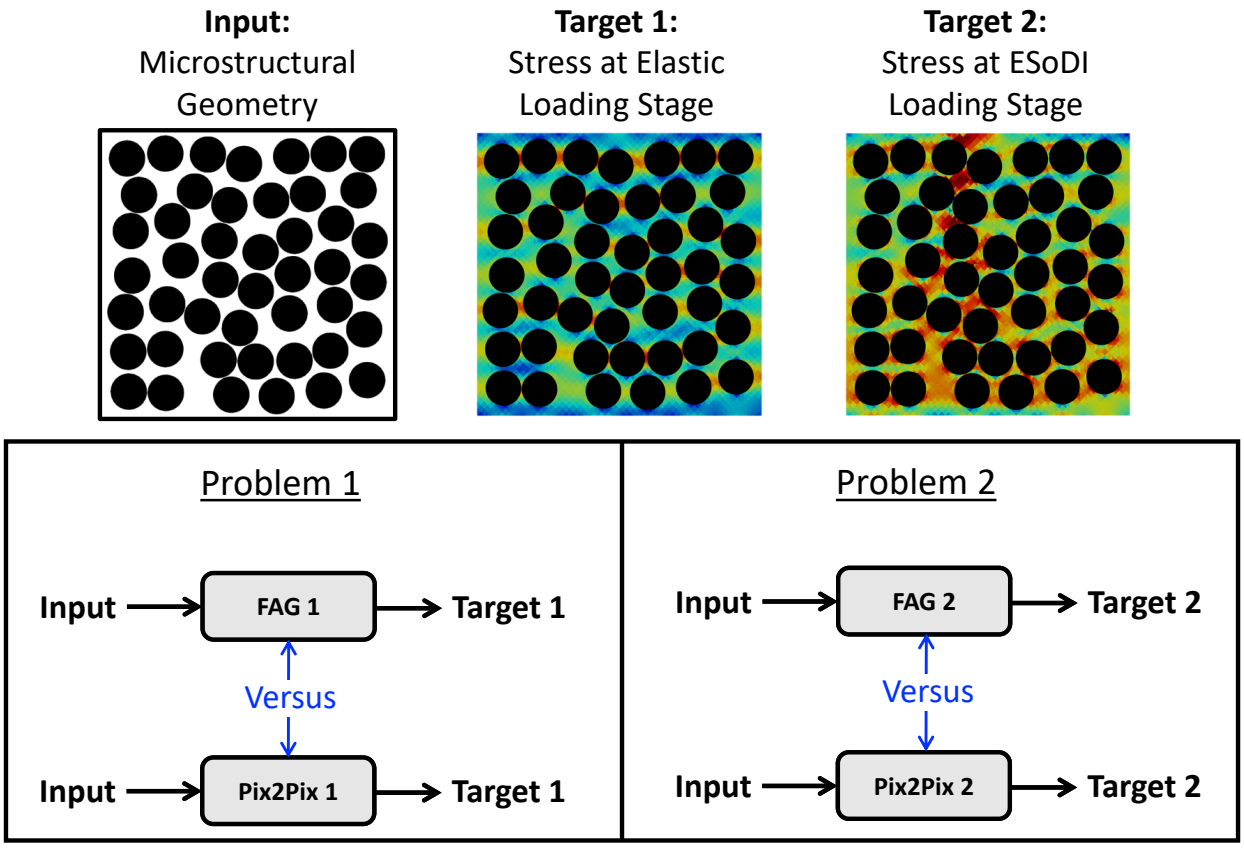

Figure 4.6: A summary of the problem studied in this research.

independent, using separately trained networks. Two different techniques, including fully convolutional generator (FCG) and Pix2Pix translation, are considered and their performances are compared. Figure 4.6 illustrates a summary of the problem that we aim to study in this research. Both methods were implemented using the TensorFlow library [1] in Python.

4.5.1 Fully Convolutional Generator

The first considered framework was a FCG to translate microstructural geometries to stress distributions. The architecture of this network was designed based on a U-Net generator. U-Net is fully convolutional network proposed by Ronneberger et al. [30] for accurate seg-

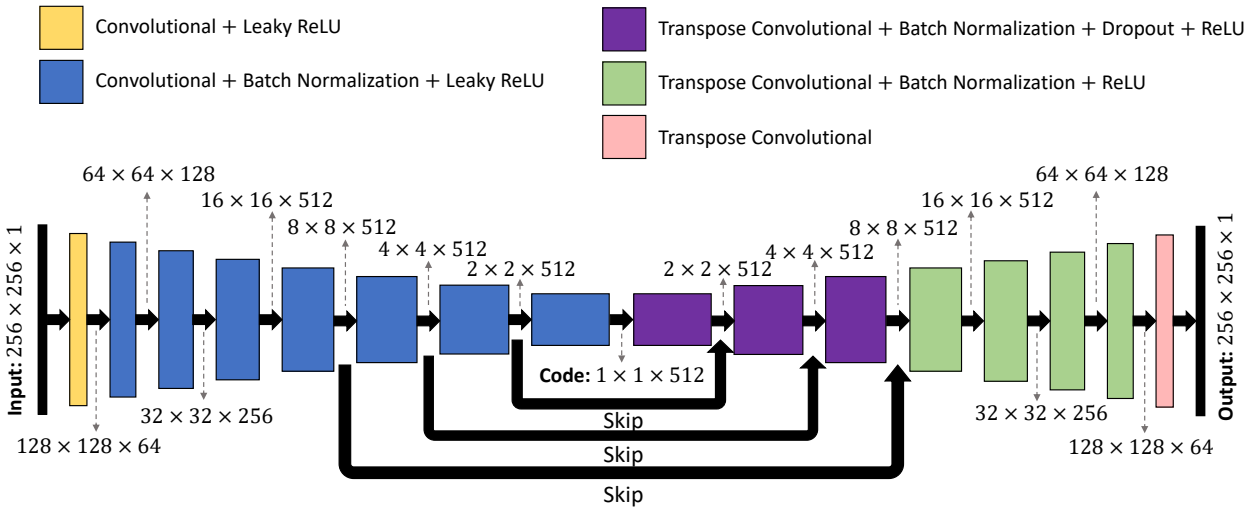

Figure 4.7: Schematic illustration of the architecture of FCG network. The same network is used for Generator in the Pix2Pix translation framework.

mentation of biomedical images. This network has been successfully applied to various image translation applications [16, 18, 39, 49]. In this work, the architecture of the U-Net generator was slightly modified so that it can generate the actual stress distribution instead of an RGB image of the stress contours.

The architecture of FCG used in this research is illustrated in Figure 4.7. The dimensions of the input and output to the network is $256 \times 256 \times 1$, consistent with those of the training data samples. The network first transforms the input into a low-dimensional vector with a dimension of $1 \times 1 \times 512$ through a series of convolutional layers. This portion of the network is called Encoder. The low-dimensional vector is called Code and contains the encoded features of the input that are the significant predictors of the output. These encoded information is then passed through a number of transpose convolutional layers, responsible to decode the encrypted features to the desired output. This portion of the network is called Decoder.

The sizes of input and output to each blocks of the FCG network is also shown with arrowed dashed-lines in Figure 4.7, with the third dimension specifying the number of applied

convolutional (or transpose convolutional) layers. Except for the first and last blocks of the FCG network, batch normalization was applied to every block. We also observed that the application of skip connections to the first three inner blocks of the network can facilitate learning, without causing an overfitting issue.

The Encoder includes eight blocks, each containing a number of convolutional layers with a kernel size of 4×4 and a stride of 2, followed by a Leaky ReLU activation function. The Decoder contains eight blocks, each contain transpose convolutional layers, followed by a ReLU activation function, except for the last block. Dropout is also applied to the first three blocks of Decoder to boost generalization and prevent overfitting. In this network, the loss is calculated using the MAE objective function.

4.5.2 Pix2Pix Translation

The image-to-image (Pix2Pix) translation method was proposed by Isola et al. [17] to translate an input image into a desired more complex representation of the input image. This approach contains two networks, namely, Generator and Discriminator. Generator is responsible to generate the desired output image based on a given input images. The Discriminator is a classifier that learns to differentiate between the target and generated images, aiming to label them as "real" and "fake", respectively.

Both the Generator and Discriminator networks are trained in an adversarial fashion. During the training epochs, first Generator is updated and tries to improve its accuracy so that it can fool Discriminator. Then, Discriminator is updated, trying to improve its performance to accurately differentiate between target and generated images. This adversarial game is repeated over and over until the Generator network is optimized.

The architectures of the Generator and Discriminator networks used in this research are

based on the ones originally proposed by the authors of the Pix2Pix translate method, Isola et al. [17]. These architectures were slightly modified to become compatible with the format of the data samples used in this research (i.e., not presented in the form of RGB images). For Generator, the FCG network, described in Section 4.5.1 and depicted in Figure 4.7, was used as its architecture.

As suggested by the authors of the Pix2Pix translation paper [17], the Discriminator's architecture was chosen to be a PatchGAN classifier. PatchGAN takes either the input and target samples, or the input and generated samples of the data set and outputs a matrix of logits. Each element of this matrix corresponds to a patch of the target (or generated) samples and its value represents the judgment of Discriminator on whether the given patch is real or fake. It must be noted that here, a probability of 1 corresponds to the class "real" while a probability 0 represents the class "fake".

The architecture of Discriminator contains six blocks of operations, as illustrated in Figure 4.8. The inputs, in the form of two $256 \times 256 \times 1$ tensors, are first concatenated to become a $256 \times 256 \times 2$ tensor in the first block. The output then passes through five blocks, each containing a number of convolutional layers, followed by batch normalization and the Leaky ReLU activation. The fifth and sixth blocks also include zero-padding. The final block (i.e., sixth block) in the architecture is a convolutional layer, responsible to transform the high-dimensional $33 \times 33 \times 512$ output of the fifth block into the low-dimensional matrix of logits with a size of $30 \times 30 \times 1$.

The Discriminator loss is calculated based on how well it can identify real patches as "real" and generated patches as "fake". Hence, the discriminator loss is the sum of two binary cross-entropy losses evaluated based on:

- Discriminator's judgment on target samples and a matrix of ones.

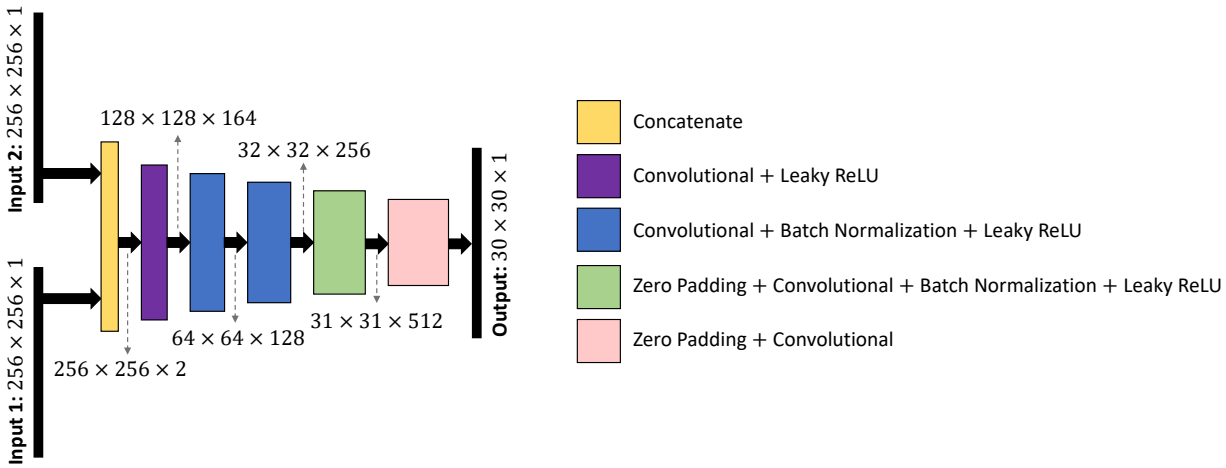

Figure 4.8: Schematic illustration of the architecture of Discriminator in the Pix2Pix translation method.

- Discriminator's judgment on generated samples and a matrix of zeros.

The Generator loss is evaluated based on how well it can fool Discriminator as well as how similar the generated samples are to the target samples. Therefore, two losses are calculated as follows:

- $\mathcal{L}_1$: Binary cross-entropy loss evaluated based on Discriminator's judgment on generated samples and a matrix of ones.
- $\mathcal{L}_2$: MAE loss evaluated based on the generated images and the corresponding target images.

The Generator loss is a weighted sum of $\mathcal{L}_1$ and $\mathcal{L}_2$ through a factor α:

$$Discriminator\ Loss = \mathcal{L}_1 + \alpha \times \mathcal{L}_2 \tag{4.1}$$

α is a hyper parameter with a default value of 100, as suggested by Isola et al. [17]. The

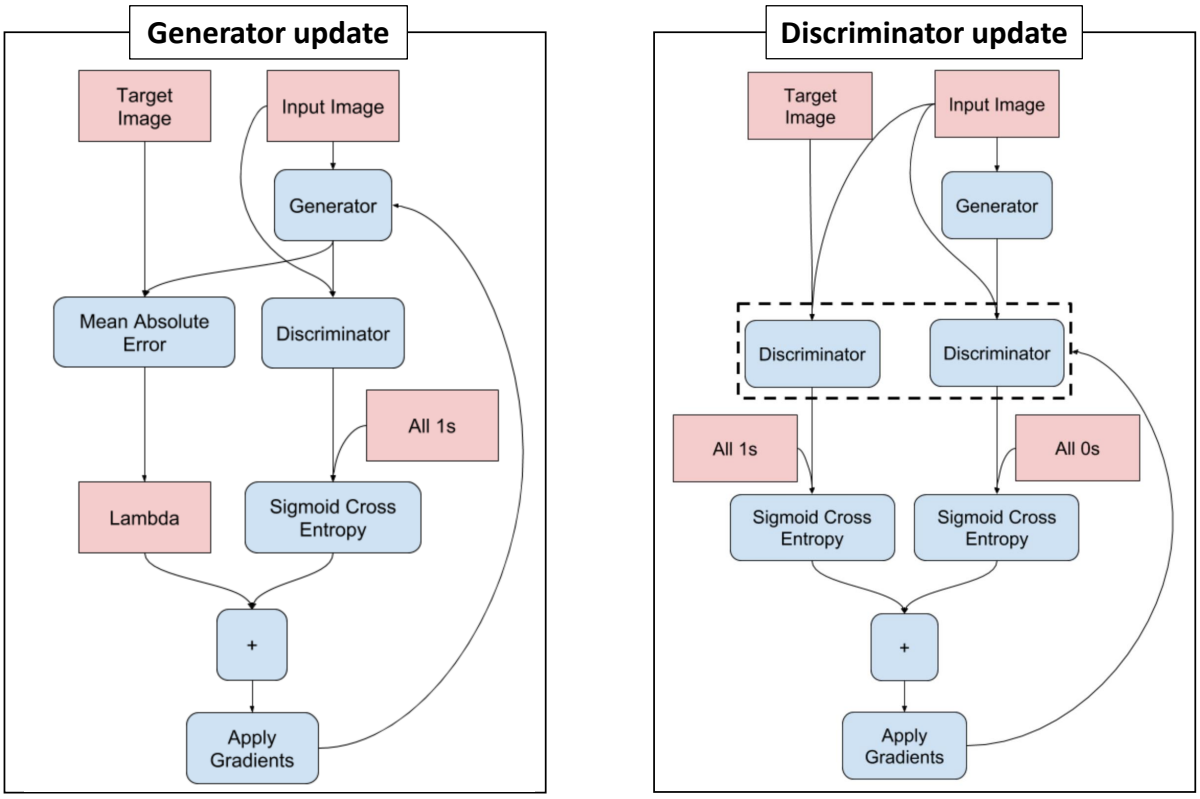

Figure 4.9: Schematic illustration of the process of updating Generator and Discriminator networks during the training (image adapted from TensorFlow [1]).

manner at which the Discriminator and Generator loses are calculate and these networks are updated are schematically illustrated in Figure 4.9.

4.6 Training and Validation

The training of the deep learning approaches described in the previous section are conducted using the Adam classifier. The training was performed using a batch size of 5 and a learning rate of 0.0002 and 200 learning epochs were applied. In order to evaluate the performance of the deep learning frameworks during the training, after the application of each epoch, the

average MAE losses of the generator based on both all the training data samples ($\mathcal{L}^{tr}_{MAE}$) and all the validation data samples ($\mathcal{L}^{val}_{MAE}$) were calculated and recorded.

As it will be explained in the next section, none of the utilized deep learning frameworks were susceptible to over-fitting due to over-training. Hence, the accuracy of the deep learning frameworks in predicting full-field stress distributions was evaluated based on the training epoch with the smallest $\mathcal{L}^{val}_{MAE}$. As a measure to reflect the correctness level of the predictions, we define and utilize a relative accuracy (RA) as follows

$$RA\ (\%) = (1 - \frac{\mathcal{L}^{val}_{MAE}}{\sigma_{max}}) \times 100 \tag{4.2}$$

where σ_{max} is the maximum recorded stress value in the FE generated results, which is equal to 10 MPa and 100 MPa for the cases of elastic and ESoDI loading stages, respectively. It must be noted that in the FE simulated stress distributions, the values of stress calculated for a small number of nodes is too large (e.g., twice greater than the maximum expected value), as a result of numerical errors. Since the number of these nodes are insignificant compared to the total number of nodes in the FE model (i.e., comprise less than 0.1% of the total nodes), they have negligible effect on the value of $\mathcal{L}^{val}_{MAE}$. However, these outlier nodes result in selecting an unrealistically large value for σ_{max}, leading to an overestimated RA. Therefore, for the evaluation of σ_{max}, the top 0.5% of nodes with largest stress values where excluded.

Chapter 5

Results

In this section, the training results are presented and the performance of the unitized deep learning frameworks in predicting full-field stress distributions at elastic and ESoDI loading stages are discussed. The training was performed using an NVIDIA V100 GPU provided by ARC at Virginia Tech. The training process of the FCG and Pix2Pix translation approaches took eight and twelve hours, respectively.

5.1 Prediction of Elastic Stress Distribution

In general, both the utilized deep learning approaches had excellent performance in predicting stress distribution at the elastic stage of loading. Figure 5.1a and Figure 5.1b illustrate the evolution of $\mathcal{L}_{MAE}^{tr}$ and $\mathcal{L}_{MAE}^{val}$ with training epochs, respectively, comparing the performances of FCG and Pix2Pix translation frameworks. As seen in the figures, both $\mathcal{L}_{MAE}^{tr}$ and $\mathcal{L}_{MAE}^{val}$ were slightly lower for the case of FCG network than those of Pix2Pix translation methods throughout the training. The highest validation RA for the cases of FCG and Pix2Pix translation approaches were 98.7% and 98.3%, at epochs 165 and 120, respectively.

Hence, the simpler method of FCG had a slightly better performance compared to the Pix2Pix translation, an advance technique. The reason is that the Discriminator network in the Pix2Pix translation approach judges the generated samples based on the trivial patterns and visual presentation. Discriminator can be thought as a person who is to visually judge

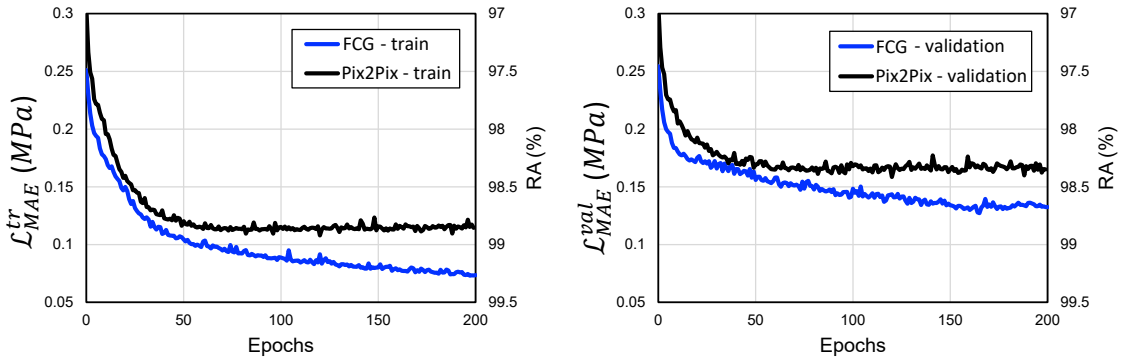

(a) (b)

Figure 5.1: Evolution of average MAE loss for the case of elastic stress distribution prediction based on (a) training data set and (b) validation data set.

the accuracy of the generated images, which is an almost impossible task. The presence of the Discriminator network merely ensures that the generated samples visually look similar to the Target samples.

Also, the performances of the frameworks were carefully monitored during the training. After the application of each epoch, a number of sample predictions were made based on the validation data set and were compared to those predicted from previous epochs. When $\mathcal{L}_{MAE}^{val}$ converged approximately after the application of 160 and 60 epochs for the cases of FCG and Pix2Pix translation approaches, respectively, the predictions became stable and no perceptible change could be visually observed as the training continued. Hence, the application of additional epochs did not cause over-fitting.

Figure 5.2 depicts sample predictions of elastic stress distribution by both FCG and Pix2Pix translation methods. As it can be seen, the generated contours by both methods are quite similar to the target stress contour and no discernible difference can be spotted. As a result, the FCG framework can be used to accurately predict the elastic stress distribution in 2-D representations of CFRP composites and there is no need to use an advanced technique i.e., Pix2Pix translation.

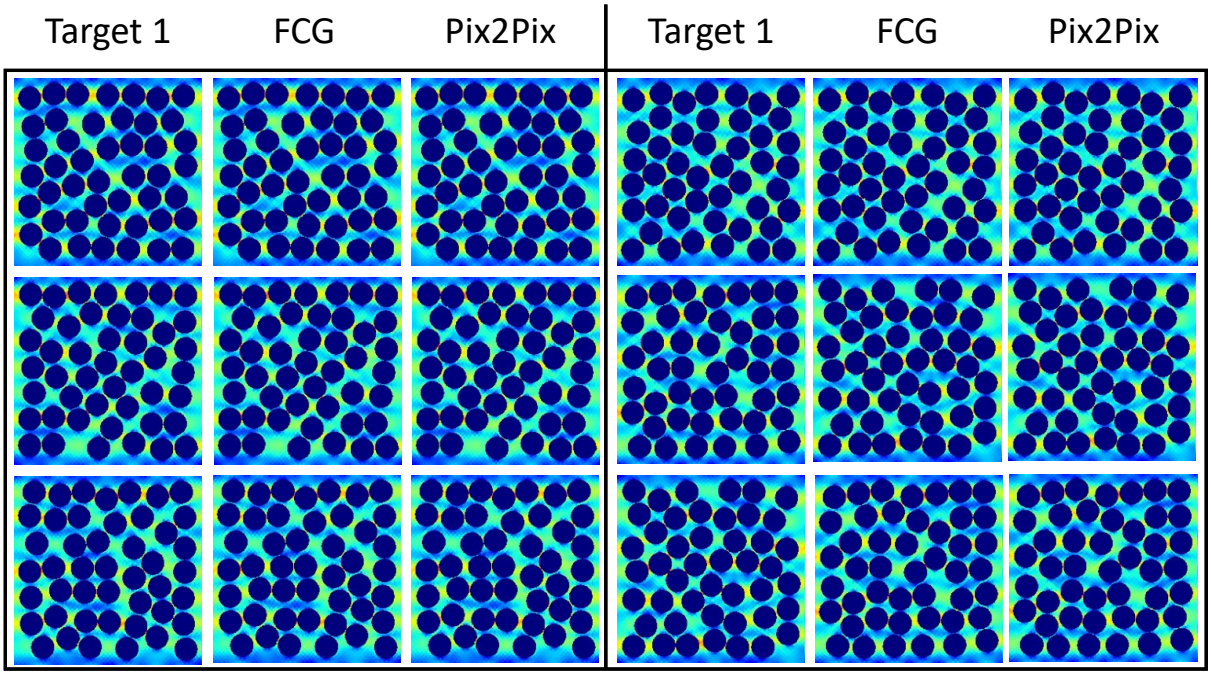

Figure 5.2: Sample elastic stress distribution predictions by FCG and Pix2Pix translation approaches.

5.2 Prediction of Stress Distribution at ESoDI

The elastic stress distribution depends more on the localized geometrical patterns of the microstructure, which can easily be captured via the convolutional layers. The stress distribution at ESoDI, on the other hand, is more dependent on the overall morphological geometry of the microstructure. Hence, predicting stress distribution at ESoDI is more complex compared to the elastic stress distribution prediction. As a result, the accuracy of stress distribution prediction at the ESoDI loading stage was lower than that of the elastic loading stage. However, the performance of the utilized deep learning approaches in predicting the stress distribution at ESoDI was still impressive.

Figure 5.3a and Figure 5.3b depicts the evolution of $\mathcal{L}_{MAE}^{tr}$ and $\mathcal{L}_{MAE}^{val}$ with training epochs, comparing the utilized FCG and Pix2Pix translation techniques. As seen in the figures, both

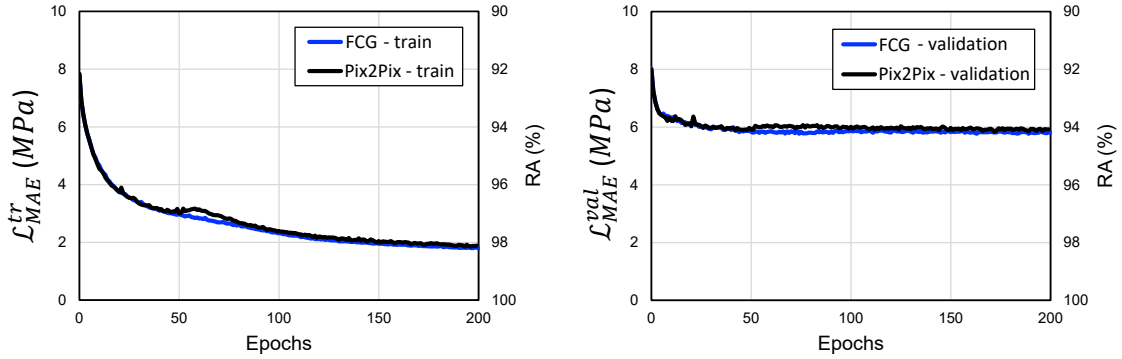

(a) (b)

Figure 5.3: Evolution of average MAE loss for the case of stress distribution prediction at the ESoDI loading stage based on (a) training data set and (b) validation data set.

methods had almost the same performance based on training and validation average MAE loses throughout the training. $\mathcal{L}^{val}_{MAE}$ for the cases of FCG and Pix2Pix translation methods converged after the application of around 50 training epochs and resulted in an RA of 94%.

Similar to the case of elastic stress distribution prediction, the presence of a Discriminator network and adversarial learning did not result in a higher accuracy. The reason was that the morphological features of the microstructure that were the significant predictors of the stress distribution at ESoDI, were complex and non-trivial.

Figure 5.4 shows sample predictions of stress distribution at ESoDI by both FCG and Pix2Pix translation approaches. As it can be seen in the figure, the predictions made by both frameworks are visually identical. As a result, the simpler method of FCG can be used to predict the stress distribution and using the more advance technique of Pix2Pix translation is not justified.

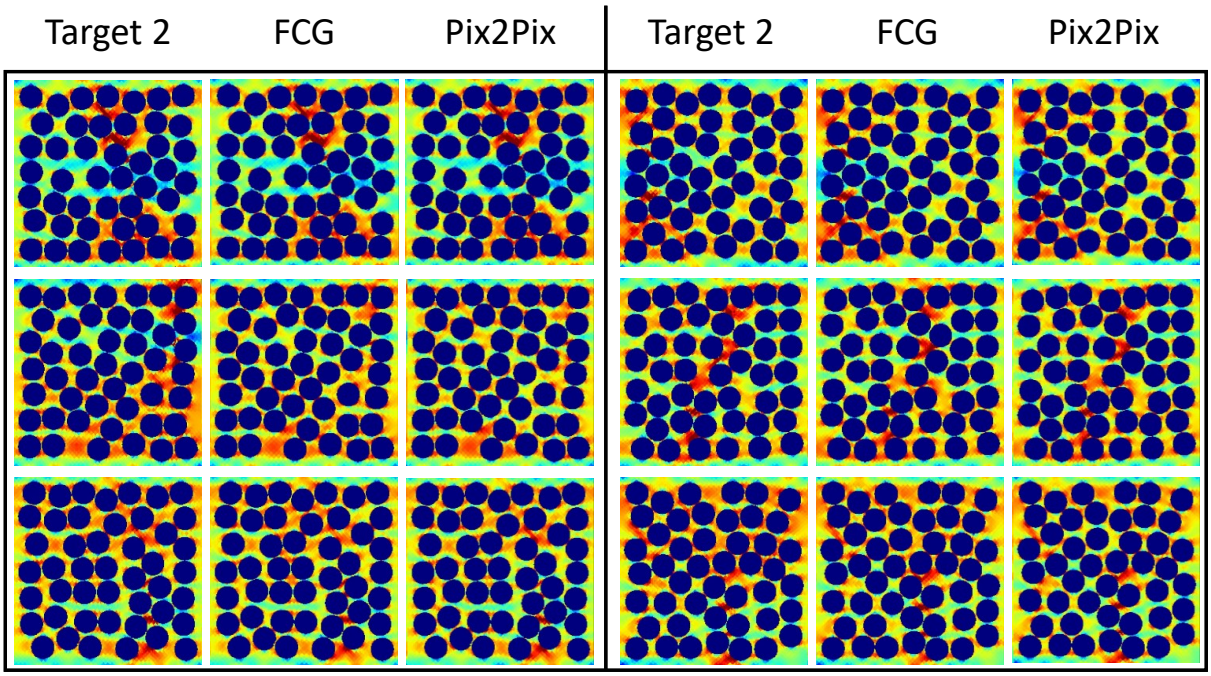

Figure 5.4: Sample stress distribution predictions at ESoDI loading stage by FCG and Pix2Pix translation approaches.

Chapter 6

Conclusions

This research proposed a framework to predict full-field stress distribution in 2-D representations of CFRP composites based on the microstructural geometry. Two different deep learning techniques, including FCG and Pix2Pix translation, were implemented within the framework and their performances were compared. The proposed framework was trained to predict the stress distributions at elastic and ESoDI stages of mechanical loading.

The implemented deep learning methods were trained and validated using a large data set, generated via FE simulations of 4500 RVEs with complex microstructural geometries. The proposed framework was trained using 4000 data samples. The performance was evaluated based on a validation data set, containing 500 samples. The relative accuracy (RA) was estimated thorough an average MAE loss, normalized by the maximum stress in the entire data set. Both the deep learning approaches (i.e., FCG and Pix2Pix translation) were able to predict the elastic stress distribution with a high RA of around 98.5%. For the more complicated problem of stress distribution prediction at ESoDI, both implemented deep learning approaches had an impressive RA of 94%. In general, both in terms of accuracy and simplicity, the FCG framework outperformed the Pix2Pix translation approach. As a result, the FCG network can be used to accurately and efficiently predict the full-field stress distribution of the microstructural representations of CFRP composites at various loading stages.

Based on the results acquired in this research, the following observations and finding can be

highlighted:

- The MAE objective function can well guide the network and the convolutional layers to learn complex and non-trivial patterns.
- The Discriminator network of the Pix2Pix translation method did not cause a higher accuracy. The results suggest that Discriminator could not contribute in guiding Generator to learn the non-trivial patterns in the specific problem studied in this thesis.

6.1 Future Work

Predicting stress distribution in microstructural representations of CFRP composites under mechanical loading is a complex problem. The complexity is due to the fact that the stress distribution, specifically in the presence of damage, depends on the non-trivial local and global geometrical patterns in the microstructure. Hence, further studies into identifying the significant predictors of the stress distributions at various loading stages through feature extraction techniques can have a significant contribution in improving the mechanical performance of the CFRP composites. Also, it is worthwhile to study the performance of the proposed framework, trained using other data sets with larger RVEs and different fiber's volume fractions. Moreover, the robustness of the proposed framework can be better evaluated by studying the sensitivity of the predictions accuracy to the RVEs' dimensions, fiber volume fraction, and fiber distribution. Additionally, other image-to-image translation techniques, such as CycleGAN [4, 6], can be utilized as the deep learning approach to study if the framework's prediction accuracy can be improved.

Bibliography

[1] M. Abadi, P. Barham, J. Chen, Z. Chen, A. Davis, J. Dean, M. Devin, S. Ghemawat, G. Irving, M. Isard, et al. Tensorflow: A system for large-scale machine learning. In *12th Symposium on Operating Systems Design and Implementation*, pages 265–283, 2016.

[2] D. W. Abueidda, Q. Lu, and S. Koric. Deep learning collocation method for solid mechanics: Linear elasticity, hyperelasticity, and plasticity as examples. *arXiv preprint arXiv:2012.01547*, 2020.

[3] M. Aliasghar-Mamaghani and A. Khaloo. Seismic behavior of concrete moment frame reinforced with gfrp bars. *Composites Part B: Engineering*, 163:324–338, 2019.

[4] A. Almahairi, S. Rajeshwar, A. Sordoni, P. Bachman, and A. Courville. Augmented cyclegan: Learning many-to-many mappings from unpaired data. In *International Conference on Machine Learning*, pages 195–204. PMLR, 2018.

[5] A. Cecen, H. Dai, Y. C. Yabansu, S. R. Kalidindi, and L. Song. Material structure-property linkages using three-dimensional convolutional neural networks. *Acta Materialia*, 146:76–84, 2018.

[6] C. Chu, A. Zhmoginov, and M. Sandler. Cyclegan, a master of steganography. *arXiv preprint arXiv:1712.02950*, 2017.

[7] M. Cid Alfaro, A. Suiker, and R. De Borst. Transverse failure behavior of fiber-epoxy systems. *Journal of Composite Materials*, 44(12):1493–1516, 2010.

[8] S. P. Donegan, N. Kumar, and M. A. Groeber. Associating local microstructure with

predicted thermally-induced stress hotspots using convolutional neural networks. *Materials Characterization*, 158:109960, 2019.

[9] Y. Dong, C. Su, P. Qiao, and L. Sun. Microstructural crack segmentation of three-dimensional concrete images based on deep convolutional neural networks. *Construction and Building Materials*, 253:119185, 2020.

[10] H. Feng and P. Prabhakar. Difference-based deep learning framework for stress predictions in heterogeneous media. *arXiv preprint arXiv:2007.04898*, 2020.

[11] E. Haghighat and R. Juanes. Sciann: A keras/tensorflow wrapper for scientific computations and physics-informed deep learning using artificial neural networks. *Computer Methods in Applied Mechanics and Engineering*, 373:113552, 2021.

[12] Y. Heider, K. Wang, and W. Sun. So (3)-invariance of informed-graph-based deep neural network for anisotropic elastoplastic materials. *Computer Methods in Applied Mechanics and Engineering*, 363:112875, 2020.

[13] L. Hernandez, R. Sepasdar, and M. Shakiba. Sensitivity of crack formation in fiber-reinforced composites to microstructural geometry and interfacial properties. In *Proceeding of the American Society for Composites, Thirty-Fifth Technical Conference*, pages 1576–1591. DEStech Publications, Inc., 2020.

[14] C. Herriott and A. D. Spear. Predicting microstructure-dependent mechanical properties in additively manufactured metals with machine-and deep-learning methods. *Computational Materials Science*, 175:109599, 2020.

[15] A. Hunter, B. A. Moore, M. Mudunuru, V. Chau, R. Tchoua, C. Nyshadham, S. Karra, D. O'Malley, E. Rougier, H. Viswanathan, et al. Reduced-order modeling through ma-

chine learning and graph-theoretic approaches for brittle fracture applications. *Computational Materials Science*, 157:87–98, 2019.

[16] N. Ibtehaz and M. S. Rahman. Multiresunet: Rethinking the u-net architecture for multimodal biomedical image segmentation. *Neural Networks*, 121:74–87, 2020.

[17] P. Isola, J.-Y. Zhu, T. Zhou, and A. A. Efros. Image-to-image translation with conditional adversarial networks. In *Proceedings of the IEEE conference on computer vision and pattern recognition*, pages 1125–1134, 2017.

[18] A. Koeppe, F. Bamer, and B. Markert. An intelligent nonlinear meta element for elastoplastic continua: deep learning using a new time-distributed residual u-net architecture. *Computer Methods in Applied Mechanics and Engineering*, 366:113088, 2020.

[19] X. Lei, L. Sun, and Y. Xia. Lost data reconstruction for structural health monitoring using deep convolutional generative adversarial networks. *Structural Health Monitoring*, page 1475921720959226, 2020.

[20] J. Mao, H. Wang, and B. F. Spencer Jr. Toward data anomaly detection for automated structural health monitoring: Exploiting generative adversarial nets and autoencoders. *Structural Health Monitoring*, page 1475921720924601, 2020.

[21] D. Mollenhauer, T. Breitzman, E. Iarve, K. Hoos, M. Swindeman, and E. Zhou. Simulation of mode i fracture at the micro-level in polymer matrix composite laminate plies. In *53rd AIAA/ASME/ASCE/AHS/ASC Structures, Structural Dynamics and Materials Conference 20th AIAA/ASME/AHS Adaptive Structures Conference 14th AIAA*, page 1651, 2012.

[22] C. B. Montgomery. *Multiscale characterization of carbon fiber-reinforced epoxy composites*. PhD thesis, University of Illinois at Urbana-Champaign, 2018.

[23] D. Mortell, D. Tanner, and C. McCarthy. In-situ SEM study of transverse cracking and delamination in laminated composite materials. *Composites Science and Technology*, 105:118–126, 2014.

[24] D. Mortell, D. Tanner, and C. McCarthy. A virtual experimental approach to microscale composites testing. *Composite Structures*, 171:1–9, 2017.

[25] M. Mozaffar, R. Bostanabad, W. Chen, K. Ehmann, J. Cao, and M. Bessa. Deep learning predicts path-dependent plasticity. *Proceedings of the National Academy of Sciences*, 116(52):26414–26420, 2019.

[26] F. Naya, C. González, C. Lopes, S. Van der Veen, and F. Pons. Computational micromechanics of the transverse and shear behavior of unidirectional fiber reinforced polymers including environmental effects. *Composites Part A: Applied Science and Manufacturing*, 92:146–157, 2017.

[27] S. Ogihara and N. Takeda. Interaction between transverse cracks and delamination during damage progress in cfrp cross-ply laminates. *Composites Science and Technology*, 54(4):395–404, 1995.

[28] K. Pazdernik, N. L. LaHaye, C. M. Artman, and Y. Zhu. Microstructural classification of unirradiated lialo2 pellets by deep learning methods. *Computational Materials Science*, 181:109728, 2020.

[29] K. Pierson, A. Rahman, and A. D. Spear. Predicting microstructure-sensitive fatigue-crack path in 3d using a machine learning framework. *JOM*, 71(8):2680–2694, 2019.

[30] O. Ronneberger, P. Fischer, and T. Brox. U-net: Convolutional networks for biomedical image segmentation. In *International Conference on Medical image computing and computer-assisted intervention*, pages 234–241. Springer, 2015.

[31] H. Saito, H. Takeuchi, and I. Kimpara. Experimental evaluation of the damage growth restraining in 90° layer of thin-ply CFRP cross-ply laminates. *Advanced Composite Materials*, 21(1):57 – 66, 2012.

[32] M. Schwarzer, B. Rogan, Y. Ruan, Z. Song, D. Y. Lee, A. G. Percus, V. T. Chau, B. A. Moore, E. Rougier, H. S. Viswanathan, et al. Learning to fail: Predicting fracture evolution in brittle material models using recurrent graph convolutional neural networks. *Computational Materials Science*, 162:322–332, 2019.

[33] T. Sebaey, G. Catalanotti, C. Lopes, and N. O'Dowd. Computational micromechanics of the effect of fibre misalignment on the longitudinal compression and shear properties of ud fibre-reinforced plastics. *Composite Structures*, page 112487, 2020.

[34] R. Sepasdar, A. Karpatne, and M. Shakiba. A data-driven approach to full-field damage and failure pattern prediction in microstructure-dependent composites using deep learning. *arXiv preprint arXiv:2104.04485*, 2021.

[35] R. Sepasdar and M. Shakiba. Micromechanical study of multiple transverse cracking in cross-ply fiber-reinforced composite laminates.

[36] M. H. Soleimani-Babakamali, R. Sepasdar, K. Nasrollahzadeh, and R. Sarlo. System-reliability based multi-ensemble of gan and one-class joint gaussian distributions for unsupervised real-time structural health monitoring. *arXiv preprint arXiv:2102.01158*, 2021.

[37] L. Sun, J. Wang, H. Hu, and A. Ni. A simplified computational strategy focused on resin damage to study matrix cracking of the cross-ply laminates under uniaxial tension load. *Materials*, 12(12):1984, 2019.

[38] N. Takeda and S. Ogihara. Initiation and growth of delamination from the tips of

transverse cracks in CFRP cross-ply laminates. *Composites science and technology*, 52(3):309–318, 1994.

[39] M. Tang, Y. Liu, and L. J. Durlofsky. Deep-learning-based surrogate flow modeling and geological parameterization for data assimilation in 3d subsurface flow. *Computer Methods in Applied Mechanics and Engineering*, 376:113636, 2021.

[40] S. Tarfan, M. Banazadeh, and M. Z. Esteghamati. Probabilistic seismic assessment of non-ductile rc buildings retrofitted using pre-tensioned aramid fiber reinforced polymer belts. *Composite Structures*, 208:865–878, 2019.

[41] J. Varna, R. Joffe, N. Akshantala, and R. Talreja. Damage in composite laminates with off-axis plies. *Composites Science and Technology*, 59(14):2139–2147, 1999.

[42] N. N. Vlassis, R. Ma, and W. Sun. Geometric deep learning for computational mechanics part i: Anisotropic hyperelasticity. *Computer Methods in Applied Mechanics and Engineering*, 371:113299, 2020.

[43] K. Wang and W. Sun. A multiscale multi-permeability poroplasticity model linked by recursive homogenizations and deep learning. *Computer Methods in Applied Mechanics and Engineering*, 334:337–380, 2018.

[44] Z. Yang, Y. C. Yabansu, R. Al-Bahrani, W.-k. Liao, A. N. Choudhary, S. R. Kalidindi, and A. Agrawal. Deep learning approaches for mining structure-property linkages in high contrast composites from simulation datasets. *Computational Materials Science*, 151:278–287, 2018.

[45] T. Yokozeki, T. Aoki, and T. Ishikawa. Transverse crack propagation in the specimen width direction of CFRP laminates under static tensile loadings. *Journal of composite materials*, 36(17):2085–2099, 2002.

[46] S. A. Zacek. Exploring the link between microstructure statistics and transverse ply fracture in carbon/epoxy composites. 2017.

[47] E. Zhang, M. Yin, and G. E. Karniadakis. Physics-informed neural networks for nonhomogeneous material identification in elasticity imaging. *arXiv preprint arXiv:2009.04525*, 2020.

[48] X. Zhang, D. R. Brandyberry, and P. H. Geubelle. IGFEM-based shape sensitivity analysis of the transverse failure of a composite laminate. *Computational Mechanics*, 64(5):1455–1472, 2019.

[49] Z. Zhou, M. M. R. Siddiquee, N. Tajbakhsh, and J. Liang. Unet++: A nested u-net architecture for medical image segmentation. In *Deep learning in medical image analysis and multimodal learning for clinical decision support*, pages 3–11. Springer, 2018.

[50] L. Zhuang, R. Talreja, and J. Varna. Transverse crack formation in unidirectional composites by linking of fibre/matrix debond cracks. *Composites Part A: Applied Science and Manufacturing*, 107:294–303, 2018.